AD-A064 784 MASSACHUSETTS INST OF TECH CAMBRIDGE DEPT OF AERONAU--ETC F/G 20/4
THE INTERACTION OF MONATOMIC AND DIATOMIC MOLECULES WITH SOLID --ETC(U)
JAN 79 L TRILLING, H Y WACHMAN, R B DOAK F44620-76-C-0036
AFOSR-TR-79-0070 NL

UNCLASSIFIED

1 OF 1

AD A064784

END

DATE FILMED

4 -79

DDC

AFOSR-TR- 79-0070
INTERIM REPORT
F44620-76-C-0036

(4) LEVEL II

THE INTERACTION OF MONATOMIC AND DIATOMIC MOLECULES WITH SOLID SURFACES

BY

LEON TRILLING, HAROLD Y WACHMAN,
ROBERT B DOAK, GIUSEPPE GOBBINI,
DAVID D DREYFUSS

MASSACHUSETTS INSTITUTE OF TECHNOLOGY
AERONAUTICS & ASTRONAUTICS DEPARTMENT
CAMBRIDGE, MA 02139

JANUARY 1979

AFOSR/NA
BOLLING AFB, DC 20332

UNCLASSIFIED

SECURITY CLASSIFICATION OF THIS PAGE (When Data Entered)

REPORT DOCUMENTATION PAGE	READ INSTRUCTIONS BEFORE COMPLETING FORM
1. REPORT NUMBER: AFOSR-TR- 79-0070	2. GOVT ACCESSION NO. / 3. RECIPIENT'S CATALOG NUMBER
4. TITLE (and Subtitle): THE INTERACTION OF MONATOMIC AND DIATOMIC MOLECULES WITH SOLID SURFACES;	5. TYPE OF REPORT & PERIOD COVERED: INTERIM rept. 1 Oct 77 — 30 Sep 78
	6. PERFORMING ORG. REPORT NUMBER
7. AUTHOR(s): LEON TRILLING, HAROLD Y. WACHMAN, GIUSEPPE GOBBINI, ROBERT B. DOAK, DAVID D. DREYFUSS	8. CONTRACT OR GRANT NUMBER(s): F44620-76-C-0036
9. PERFORMING ORGANIZATION NAME AND ADDRESS: MASSACHUSETTS INSTITUTE OF TECHNOLOGY, AERONAUTICS & ASTRONAUTICS DEPARTMENT, CAMBRIDGE, MA 02139	10. PROGRAM ELEMENT, PROJECT, TASK AREA & WORK UNIT NUMBERS: 2307A3, 61102F, A3
11. CONTROLLING OFFICE NAME AND ADDRESS: AIR FORCE OFFICE OF SCIENTIFIC RESEARCH/NA, BLDG 410, BOLLING AIR FORCE BASE, D C 20332	12. REPORT DATE: Jan 79
	13. NUMBER OF PAGES: 31
14. MONITORING AGENCY NAME & ADDRESS (if different from Controlling Office): 33p.	15. SECURITY CLASS. (of this report): UNCLASSIFIED
	15a. DECLASSIFICATION/DOWNGRADING SCHEDULE

16. DISTRIBUTION STATEMENT (of this Report)

Approved for public release; distribution unlimited.

17. DISTRIBUTION STATEMENT (of the abstract entered in Block 20, if different from Report)

18. SUPPLEMENTARY NOTES

19. KEY WORDS (Continue on reverse side if necessary and identify by block number)

MONATOMIC MOLECULES
DIATOMIC MOLECULES
SOLID SURFACES

20. ABSTRACT (Continue on reverse side if necessary and identify by block number)

The research conducted under contract F44620-76-C-0036 in the year 1978 is well described by the three papers presented at the XIth International Symposium on Rarefied Gas Dynamics. We submit them in lieu of an interim scientific report.

DD FORM 1473

220 003

ANNUAL REPORT
Contract Number F44620-76-C-0036
January 5, 1979

The results of our research in the first eight months of the contract year 1977-78 are summarized in the three attached papers which were presented at the 11th International Symposium in Rarefied Gas Dynamics. Two of them will appear in the Symposium proceedings.

Theoretical research has since proceeded in two directions:

(1) The model presented by Trilling for spherical droplets of continuous material is generalized to other geometrical configurations. Since ice crystals appear to grow as hexagonal platelets it has appeared interesting to consider the growth of flat circular cylinders ($R >> h$ where R is the cylinder radius and h is its height). The rate of growth on the sides turns out to be sufficiently faster than on the circular faces to explain why a thin pillbox does not grow into a sphere. The rate of growth is fastest near sharp edges and therefore edges are not smoothed out.

(2) Some further extension of the statistical mechanics of nucleation embryos beyond the enclosed paper by Gobbini appear in his S.M. Thesis. However, to our great regret, Gobbini has now left this project to do his doctoral research in another field, and we are seeking a replacement for him to continue the statistical theory.

Experimental research beyond the results of the symposium paper has necessitated some rather extensive rebuilding of our experimental apparatus. In particular we have been in the process of reconstructing the molecular beam source chamber, and the target mount assembly. Extensive experimental measurements on the scattering of beams of water vapor from ice and Covellite surfaces have confirmed and extended earlier results obtained in our laboratory by A. Swartzon.

Mass Distribution of Droplets in Nucleation

Leon Trilling*

Massachusetts Institute of Technology

ABSTRACT

We present a general model for the interaction of a specified distribution of water droplets with a supersaturated atmosphere. In terms of an intrinsic nucleation time scale, the evolution of the droplet size distribution is obtained explicitly as a function of the initial state and of the rate of formation of new nuclei. The connection between the intrinsic nucleation time scale and real time is then found by solving the bulk conservation equations for the atmosphere with the condensation as an energy source term. Examples are worked out for an initially uniform droplet distribution for various rates of nucleus formation.

In a number of condensation problems of practical importance, it is useful to know the mass distribution of droplets or crystallites as condensation proceeds. Depending on the order of that mass, the problem is best approached by means of molecular kinetics and statistical mechanics (particles of up to a few thousand molecules in a rarefied vapor or gas vapor mixture) or as a two phase continuum non-equilibrium thermodynamics problem (solid or liquid nuclei of order 0.1 to 10 microns). In the latter case, the mean free path of the vapor or gas-vapor mixture may be large or small compared to the diameter of the nucleus.

The statistical mechanics of small crystallites ($\sim 10^2$ to 10^5 atoms) interacting with their vapor raises two difficult questions - What is the frequency distribution of their configurations in phase space? What is the energy (particularly the vibrational energy) to be ascribed to any given configuration? The first of these questions can now be answered fairly well (see for example F. Abraham [1] or the paper submitted to this symposium by G. Gobbini [2]). The answer to the second is still subject to considerable argument, and depends on the model chosen for the crystallite. Such

*Professor of Aeronautics and Astronautics
Massachusetts Institute of Technology
Cambridge, Massachusetts

models require either a definite set of rules for individual molecular interactions or a convincing way of relating the behavior of small assemblages to that of the material in the bulk.

If the nucleus is large enough (a diameter of 0.1 micron corresponds to some 10^8 atoms) it is usually represented as a solid or liquid sphere whose main properties (e.g. surface tension, chemical potential) are those of the material in the bulk. Because its mass is large, it behaves in collisions with ambient molecules of vapor or gas as a body at rest.

The nucleating particle size distribution in a non-equilibrium situation is governed by a supply process, a growth (or decay) rate which depends on the degree of background saturation, on the fluid mechanics and surface physics of interactions with the background, and on an exhaustion process which removes particles from the field at a rate which depends on particle size.

We discuss the nucleation of water droplets (supplied for example by an aircraft jet exhaust or some other device) in a supersaturated atmosphere of specified initial properties, under conditions (e.g. initial droplet size) which makes re-evaporation sufficiently rare to be negligible.

Let the ambient vapor density be ρ_v and the corresponding saturation density be ρ_{v_0}; then the saturation ratio is defined as:

$$S = 1 - \frac{\rho_{v_0}}{\rho_v} \quad ; \quad \frac{dS}{dt} = \frac{\rho_{v_0}}{\rho_v^2} \frac{d\rho_v}{dt} - \frac{1}{\rho_v} \frac{d\rho_{v_0}}{dt} \qquad (1)$$

and ρ_{v_0} is related to the ambient temperature T by the Clausius Clapeyron equation:

$$\frac{d\rho_{v_0}}{dt} = \frac{\rho_{v_0}}{T} \left(\frac{L}{kT} - 1 \right) \frac{dT}{dt} \qquad (2)$$

where L is the latent heat of condensation per molecule.

If the vapor molecules and the droplets or crystals are convected by the surrounding air motion, then, applying the continuity equation, for both air and vapor, to eliminate the divergence of the velocity vector, we obtain

$$\frac{d}{dt} \left(\frac{\rho_v}{\rho_a} \right) = - \frac{I}{\rho_a} \qquad (3)$$

where I is the total rate of condensation of the vapor per unit volume and unit time and ρ_a is the air density. We write the energy conservation equation for the ambient air under the assumption that the heat released by condensation is fully transmitted to the air (e.g. $\rho_v/\rho_a << 1$)

$$\rho_a c_{p_a} \frac{dT}{dt} = \frac{d\rho_a}{dt} + LI \qquad (4)$$

This, with the (ideal gas) equation of state for air eliminates the temperature and density from (1-3); finally eliminating $d\rho_{v_0}/dt$ by use of (2), we obtain:

$$\frac{1}{1-S}\frac{dS}{dt} = \left(1 - \frac{\gamma-1}{\gamma}\frac{L}{kT}\right)\frac{d(\log p_a)}{dt} - \frac{I}{\rho_v}\left(1 + \frac{\rho_v}{\rho_a}\frac{\gamma-1}{\gamma}\left(\frac{L}{kT}\right)^2\right) \qquad (5)$$

This is the bulk equation which connects the saturation ratio history to the dynamics of the bulk air motion and to the total vapor condensation rate. A similar derivation may be found in [3].

If we now represent the condensed phase as a distribution of spherical clusters f(r,t) where f(r,t) is the number of clusters per unit volume whose radius is in the range (r,r + dr), then the condensation rate I is

$$I = 4\pi\rho_L \int_0^\infty r^2 f(r,t)\frac{dr}{dt}\,dr \qquad (6)$$

The continuity equation for the cluster size density in (r,t) space is

$$\frac{\partial f}{\partial t} + \frac{\partial}{\partial r}\left(f\frac{dr}{dt}\right) = \Psi(r,t) \qquad (7)$$

where $\Psi(r,t)$ is the rate per unit volume per unit time at which new nuclei of mass (r, r+dr) appear in the fluid.

Finally, we balance the energy transferred to a droplet by collision with ambient gas molecules (or by convection) and the energy exchanged in the condensation process, and obtain a relation of the form:

$$\frac{dr}{dt} = F(r,s) = sv(r) \qquad (8)$$

When the time scale of collisions is short compared to the time scale for droplet growth as, in the Stokes flow regime, Fukuta

and Walter [4], and independently Sedunov[3], obtain

$$\rho_L \frac{dr}{dt} = \frac{\mu_a S}{Ar + Bh} \tag{9a}$$

$$\text{with } A = \frac{\rho_a}{\rho_{v_0}} \bar{S} + \frac{\gamma-1}{\gamma} \frac{m_v}{m} Pr \left(\frac{L}{kT}\right)^2 \tag{9b}$$

$$Bh = \frac{\rho_a}{\rho_{v_0}} \bar{S} \ell_\beta + \frac{\gamma-1}{\gamma} \frac{m_v}{m_a} Pr \left(\frac{L}{kT}\right)^2 \ell_\alpha \tag{9c}$$

$$\ell_\alpha = \frac{2\gamma Pr^{-1} \mu_a}{\alpha(\gamma-1)\rho_a} \sqrt{\frac{2\pi m_a}{kT}} \qquad \ell_\beta = \frac{D_{av}}{\beta} \sqrt{\frac{2\pi m_v}{kT}} \tag{9d}$$

Here μ_a is the viscosity of the air

D_{av} is the diffusion coefficient of water vapor in air

m_v, m_a are the molecular masses of vapor and air respectively

h is a characteristic length, essentially a Knudsen layer thickness

Pr is the Prandtl number of air $Pr = \mu C_p/k$

$\bar{S}$ is the Schmidt number of air $\bar{S} = \mu/\rho_a D_{av}$

α is the energy accommodation coefficient for air on water

β is the condensation coefficient

The equivalent result for the free molecule regime is:

$$\rho_L \frac{dr}{dt} = \frac{\alpha\beta S \rho_v C_v}{\alpha + \beta \frac{\rho_v C_v}{\rho_a C_a} \left(\frac{L}{kT}\right)^2} \tag{10}$$

Note that ℓ_α, ℓ_β and h are lengths of the order of the mean free path of the gas; A, B are numbers of order unity. We expect (9) to hold since the Reynolds number

$$\rho_a \frac{r\, dr/dt}{\mu_a}$$

is of order $\rho_a S/\rho_L$ which is well below unity when the radius of the droplet is larger than the mean free path. In air at sea level, the mean free path of air is of order 0.1 microns; one would therefore use (9) for all droplets considered there. But at an altitude of 50 km, the mean free path is 100 microns and formula (10) is more appropriate.

Substituting (8) into (9) or (10) and introducing the new coordinates

$$\frac{1}{S}\frac{\partial}{\partial t} = \frac{\partial}{\partial \tau} \quad ; \quad v\frac{\partial}{\partial r} = \frac{\partial}{\partial \sigma} \quad ; \quad vf = g \qquad (11)$$

we obtain

$$\frac{\partial g}{\partial \tau} + \frac{\partial g}{\partial \sigma} = \frac{v(\sigma)}{s(\tau)} \quad \Psi(r,t) = \psi(\sigma,\tau) \qquad (12)$$

which is integrated formally to give

$$g(\sigma,\tau) = g_0(\sigma-\tau) + \int_0^{\tau} \psi(\zeta+\sigma-\tau,\ \zeta)\, d\zeta \qquad (13)$$

where $\frac{g_0(\sigma)}{v_0(\sigma)}$ is the initial distribution of droplet sizes.

Thus, in the absence of a source of nuclei, g shifts to the right; the distribution function keeps its shape but is applied to larger droplets; the droplets in the system grow and the distribution function scale is modulated by the factor v_0/v (see 11c) which is generally greater than unity. The time scale τ is not real time; it is related to the saturation ratio by (11a) and as $S \to 0$, t approaches a finite value while $\tau \to \infty$; when the droplets have condensed all the available vapor, they grow no further.

If a source term is specified [e.g. $\Psi(r,t)$], the form of $\psi(\sigma,\tau)$ is not known since (11a) cannot be inverted without solving (5); but its role is clear; it provides new nuclei which compete with the original ones in $g_0(\sigma)$ for available vapor and therefore inhibit the growth of large droplets by drawing some vapor to new nuclei. As a result, the condensation process is completed sooner in real time.

To complete the formal solution of the problem, we substitute (13) into (5) transformed to the τ coordinate:

$$\frac{d\ \log(1-S)}{dt} + \left(1 - \frac{\gamma-1}{\gamma}\frac{L}{kT}\right)\frac{d\ \log p_a}{dt} = \left[1+\frac{\rho_v}{\rho_a}\frac{\gamma-1}{\gamma}\left(\frac{L}{kT}\right)^2\right]x \qquad (14)$$

$$x\ \frac{4\pi\rho_L}{\rho_{v_0}} \int r^2(\sigma)g(\sigma,\tau)v(\sigma)d\tau$$

Remembering the definition of S, we eliminate ρ_v from (14), since $1-S = \frac{\rho_{v_0}}{\rho_v}$. Thus

$$\frac{d \log(1-S)}{dt} + \left(1 - \frac{\gamma-1}{\gamma}\frac{L}{kT}\right)\frac{d \log p_a}{dt} = \left[(1-S) + \frac{\rho_{v_0}}{\rho_a}\frac{\gamma-1}{\gamma}\left(\frac{L}{kT}\right)^2\right]$$

$$\frac{4\pi\rho_L}{\rho_{v_0}} \int_0^\infty r^2(\sigma)\left[g_0(\sigma-\tau) + \int_0^\tau \psi(\zeta + \sigma-\tau,\zeta)\, d\zeta\right] v\, d\sigma \qquad (14a)$$

Let I_1 denote the integral of the homogeneous part of the solution and I_2 that of the non-homogeneous part. In the special case of an atmosphere at rest $d \log \rho_a/dt$ vanishes, and in terms of I_1 and I_2,

$$\frac{\rho_a}{\rho_{v_0}}\frac{\gamma}{\gamma-1}\left(\frac{kT}{L}\right)^2\left[\frac{1}{1-S} - \frac{1}{(1-S) + \frac{\rho_{v_0}}{\rho_a}\frac{\gamma-1}{\gamma}\left(\frac{L}{kT}\right)^2}\right]\frac{d(1-S)}{dt} =$$

$$= \frac{4\pi\rho_L}{\rho_{v_0}}\,(I_1 + I_2) \qquad (14b)$$

Integrating (14b)

$$S = \left\{(1-S_i)\left(1+\frac{\rho_{v_0}}{\rho_a}\frac{\gamma-1}{\gamma}\left(\frac{L}{kT}\right)^2\right)e^{\frac{4\pi\rho_L}{\rho_a}\frac{\gamma-1}{\gamma}\left(\frac{L}{kT}\right)^2\int_0^\tau [I_1(\tau)+I_2(\tau)]d\tau} - \right.$$

$$\left. - \left(1-S_i+\frac{\rho_{v_0}}{\rho_a}\frac{\gamma-1}{\gamma}\left(\frac{L}{kT}\right)^2\right)\right\} x$$

$$x\left\{(1-S_i)e^{\frac{4\pi\rho_L}{\rho_a}\frac{\gamma-1}{\gamma}\left(\frac{L}{kT}\right)^2\int_0^\tau [I_1(\tau)+I_2(\tau)]d\tau} - \right.$$

$$\left. - \left(1-S_i+\frac{\rho_{v_0}}{\rho_a}\frac{\gamma-1}{\gamma}\left(\frac{L}{kT}\right)^2\right)\right\}^{-1} \qquad (15)$$

where S_i is the initial supersaturation. Whenever the exponent of the exponential is positive, $S < S_i$, and as the exponent increases, S decreases monotonically toward zero.

The real time variable t is obtained by integrating (11a) when $S(\tau)$ is known. In particular, saturation occurs when S vanishes, or

$$\int_0^{\tau_S} [I_1(\tau) + I_2(\tau)]d\tau = \frac{\gamma\rho_a}{4\pi(\gamma-1)\rho_L} \left(\frac{kT}{L}\right)^2 \log \frac{1-S_i + \frac{\rho_{v_0}}{\rho_a}\frac{\gamma-1}{\gamma}\left(\frac{L}{kT}\right)^2}{(1-S_i)\left(1 + \frac{\rho_{v_0}}{\rho_a}\frac{\gamma-1}{\gamma}\left(\frac{L}{kT}\right)^2\right)} = \tag{16}$$

$$= \frac{\gamma\rho_a}{4\pi(\gamma-1)\rho_L} \left(\frac{kT}{L}\right)^2 \log \left[1 + \frac{\frac{\rho_{v_0}}{\rho_a}\frac{\gamma-1}{\gamma}\left(\frac{L}{kT}\right)^2 S_i}{(1-S_i)\left(1 + \frac{\rho_{v_0}}{\rho_a}\frac{\gamma-1}{\gamma}\left(\frac{L}{kT}\right)^2\right)}\right]$$

since $\frac{\gamma-1}{\gamma}\frac{\rho_{v_0}}{\rho_a} \ll 1$ for most problems of practical interest, (16) may be approximated as

$$\int_0^{\tau_S} [I_1(\tau) + I_2(\tau)]d\tau \simeq \frac{\rho_{v_i}-\rho_{v_0}}{4\pi\rho_L} \simeq \frac{S_i}{4\pi}\frac{\rho_{v_i}}{\rho_L} \tag{17}$$

where ρ_{v_i} is the initial ambient vapor pressure and ρ_{v_0} the saturation vapor pressure at the (constant) ambient temperature. The integrals $I_1(\tau)$ and $I_2(\tau)$ represent the contributions of the growth of original droplets and added source droplets respectively to the depletion of the available vapor supply. The integral I_1 can be computed explicitly when the original distribution of droplet size $f_0(r)$ and the growth law (8) are known. The integral I_2 includes $\psi(\sigma,\tau)$ and cannot be computed directly from $\psi(r,t)$. But a step by step numerical integration where I_2 is evaluated approximately over the nth step by using the value of S_{n-1}, gives a good approximate result in a straightforward manner.

For Stokes flow (9), a convenient non-dimensional time $\bar{\tau}$ based on the rate of growth of a reference droplet of radius r_0 is introduced:

$$\bar{\tau} = \frac{\mu_a \tau}{\rho_L r_0 (Ar_0 + Bh)} \tag{18a}$$

For a 1 micron droplet at sea level, one unit in $\bar{\tau}$ corresponds to 100 seconds. Similarly a scale for the distribution function is introduced:

$$\eta = \frac{4\pi\rho_L r_0^3 f_0}{\rho_{v_0}} \tag{18b}$$

That is essentially the ratio of mass of condensed material to the mass of vapor at saturation conditions in the same volume. For a set of droplets of size r_0, the integral $\int I_1 dt$ is evaluated as

$$\int I_1 \, dt = \eta(\bar{\tau} + \bar{\tau}^2) \tag{19a}$$

and the integral $\int I_2 d\tau$ becomes:

$$\int I_2 d\tau = \xi \int \bar{t} \, d\bar{\tau} \quad ; \quad \xi = \frac{4\pi\rho_L}{\rho_{v_0}} \frac{r_0^3 \Psi (Ar + Bh)}{r_0} \tag{19b}$$

where ξ is the non-dimensional source intensity defined in a manner comparable with η and $\bar{t}$ is a non-dimensional "real time" compatible with $\bar{\tau}$. The effect of the source term is shown on Figures 1, 2 by comparing the real time histories of the condensation for $\eta = 1$, $\xi = 0,1,5$ for an initially uniform set of droplets r_0.

This research was supported by the U.S. Air Force Office of Scientific Research under contract # F44620-76-C-0036.

REFERENCES

1. F.F. Abraham: Homogeneous Nucleation Theory, Academic Press, N.Y. (1974).

2. G. Gobbini: "A Contribution to the Statistical Mechanics of Homogeneous Nucleation," (11th RGD Symposium - Cannes 1978)
also, "Homogeneous Nucleation of Liquifying or Sublimating Gases," S.M. Thesis - M.I.T., June 1978 - 94 pp.

3. Y.S. Sedunov: Physics of Drop Formation in the Atmosphere, J. Wiley and Sons, N.Y. (1974).

4. N. Fukuta & L.A. Walter: "Kinetics of Hydro-meteor Growth from a Vapor-Spherical Model," J. Atm. Sc., Vol. 27, pp. 1160-1172, Nov. 1970.

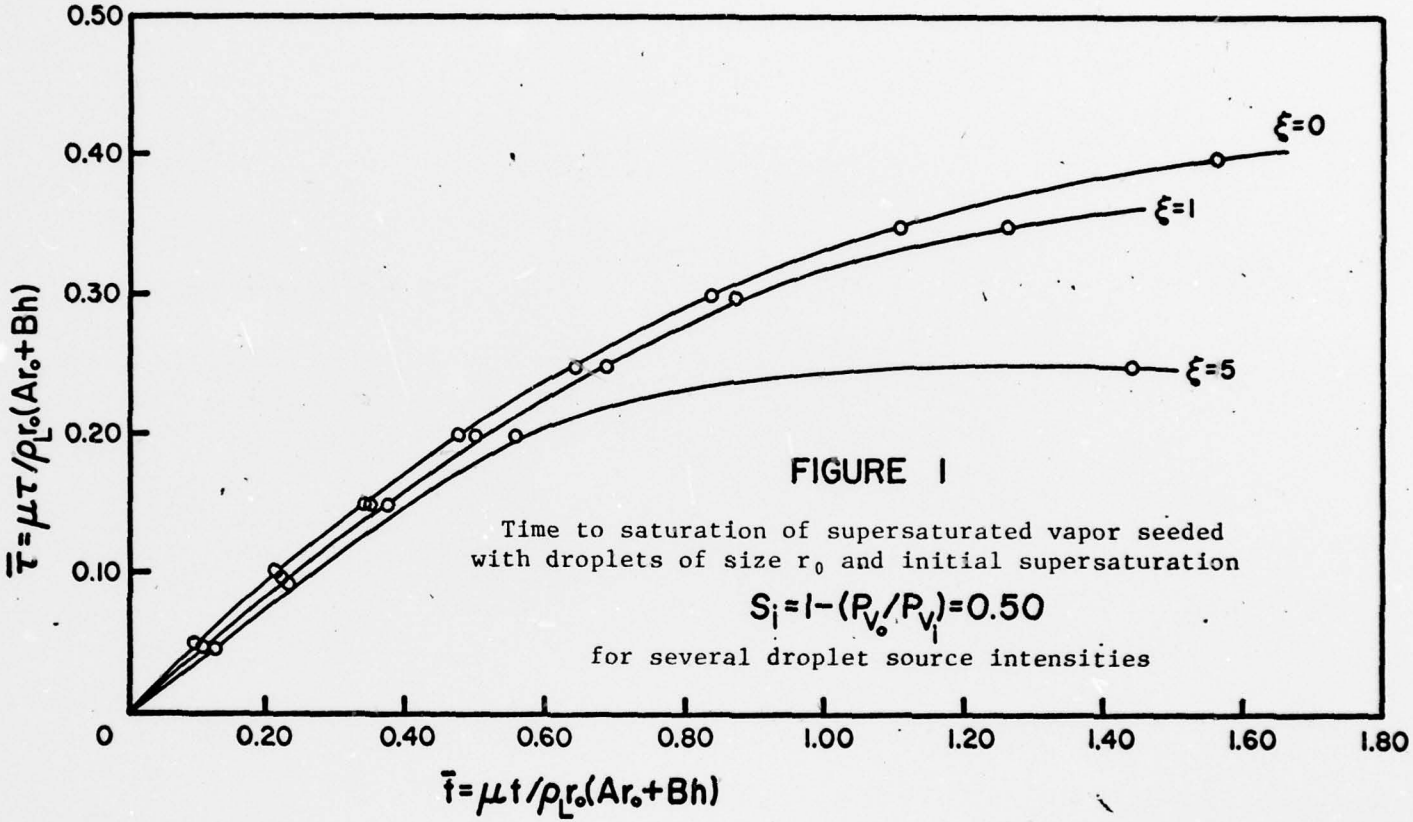

FIGURE 1

Time to saturation of supersaturated vapor seeded with droplets of size r_0 and initial supersaturation

$S_i = 1-(P_{V_o}/P_{V_i})=0.50$

for several droplet source intensities

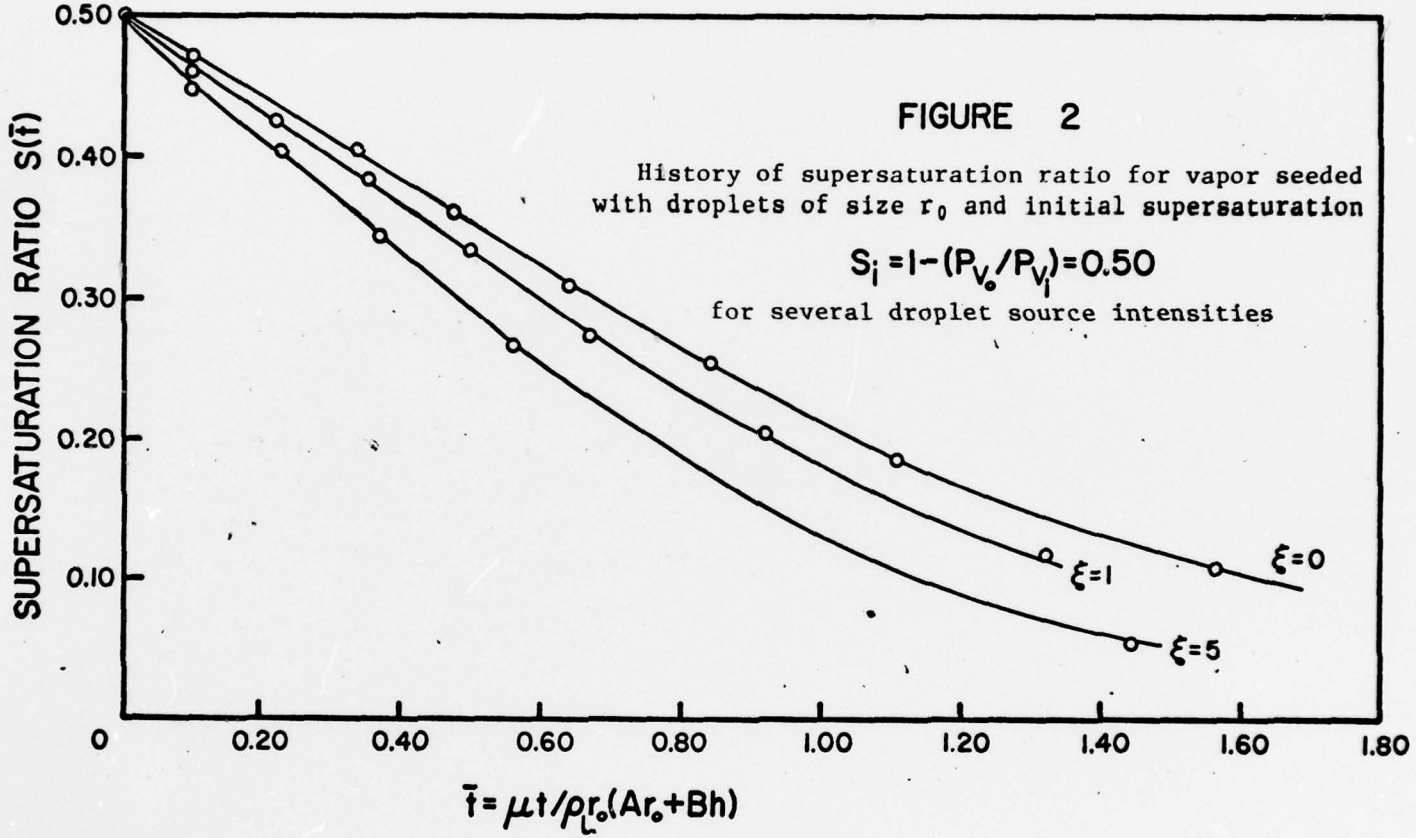

FIGURE 2

History of supersaturation ratio for vapor seeded with droplets of size r_0 and initial supersaturation

$S_i = 1-(P_{V_o}/P_{V_i}) = 0.50$

for several droplet source intensities

A CONTRIBUTION TO THE STATISTICAL MECHANICS OF HOMOGENEOUS NUCLEATION

Giuseppe Gobbini*
Massachusetts Institute of Technology

ABSTRACT

Homogeneous nucleation depends on the free energy of condensational embryos, an important part of which depends, in its turn, on the embryos' natural frequencies of vibration. Mathematical models previously proposed for these vibrations are discussed, then a new one is proposed, which envisages both compressional and distortional vibrations. This model is applied to small cubic crystallites, and the resulting values of free energy, obtained by means of numerical computation, are presented and discussed.

It is well known that the liquefaction or sublimation of a gas is severely delayed when there are no pre-existing nuclei on whose surface condensation may begin. Under such conditions, the supersaturated gas is believed to build embryonic aggregations, or clusters. For smaller clusters,[1] free energy increases with size, and so these clusters tend to decay. Above a critical size, however, free energy decreases with size. When supercritical clusters are formed, they tend to grow, and condensation finally occurs.

The free energy of a cluster made of n molecules is:

$$f_n = -kT \ln(Q_n e\, m^n / N_n)$$

where m: total number of molecules in the enclosure
N_n: number of clusters made of n molecules

and: $Q_n = (n!)^{-1} \int \exp(-H_n/kT)\, d\bar{x}\, d\bar{p}$

where H_n is the Hamiltonian of the cluster, $\bar{x}$ and $\bar{p}$ its Lagrangian position and momentum coordinates. If we suppose the clusters to be crystallites, with their molecules oscillating around invariable lattice positions, H_n, and therefore Q_n and f_n, can be decomposed into the sum of terms due to translational, rotational, vibrational and binding energy. The vibrational contribution to free energy can be expressed, if the temperature is not too low, by the formula:

$$(1) \quad f_{n,\,vib} = (3n-6)kT \ln \frac{h}{kT} + kT \ln \prod_{i=1}^{3n-6} \omega_{ni}$$

*Graduate Student, Massachusetts Institute of Technology
Dept. of Aeronautics & Astronautics; Cambridge, MA. 02139 USA

where the ω_{ni}'s are the 3n-6 natural frequencies (in rad/sec) of a crystallite of n molecules. It has been pointed out[2] that the "replacement" term of free energy lies within this component.

An expression for the intermolecular potential is necessary in order to find the natural frequencies. Two different kinds of expressions have been proposed so far, to my knowledge. One is a potential depending only on the distance between nearest neighbors. If the problem is linearized, this means modeling the crystallite as mass points collegated by ideal coil springs. A serious objection must be raised against this model: it works for a f.c.c. lattice - to which it was applied by Hoover et al.[3] - but would not work for most other lattices. In most crystalline lattices non-rigid deformations are possible, which leave the distance between nearest neighbors unchanged; the model provides no restoring force for such deformations.

The directionality of bonds, which holds these lattices together, was taken into account in the potential proposed by Stillinger and Rahman for liquid water[4,5]. The water molecule was modeled as a rigid tetrahedron with four electrical charges at the corners, and the potential was the sum of a term depending on the distance between centers and of the electrostatic terms. The motions allowed were compressions and librations - the latter being rigid rotations of a molecule with respect to its neighbors. If a model like this were applied to a crystallite, it would account for the stability of any kind of lattice, but would probably envisage unrealistic vibrational modes. The assumption of molecular rigidity is too strict. In the very case considered in ref.[4,5], water, the equilibrium angle between valence orbitals changes of about 5% from the water vapor molecule to the perfect ice crystal. It is only reasonable to assume that oscillations of this angle around its equilibrium value occur in crystallites. On the other hand, allowing librational freedom to molecules is probably too liberal an assumption for crystalline aggregates, where bonds are complete and fairly tight, while it seems correct for a liquid, where bonds are incomplete, strained and easily broken.

For these considerations, a different linear model of crystalline lattices is proposed here. It is supposed that molecules are not rigid, but that their valence orbitals always stay oriented toward the centers of nearest neighbors. Librations, i.e., rigid rotations of a molecule, are therefore excluded. The displacement of a molecule from its equilibrium position will cause a change both of the distance between

centers and of the angle between orbitals. Both are opposed by a restoring force, so that compressional and distortional vibrations result. Let us call K_c and K_d the elastic constants of compression and distortion, respectively; d_{ij} the distance between the centers of the i-th and the j-th molecule; α_{ijk} the angle with vertex in the center of the i-th molecule and sides going through the centers of the j-th one and of the k-th one; $d^0_{ij} = d$ and α^0_{ijk} the respective equilibrium values. The small-displacement potential will be:

$$\Phi = \frac{1}{2} \sum_{1}^{n}{}_i \sum_{\tilde{i}}{}_j K_c (d_{ij} - d^0_{ij})^2 + \frac{1}{2} \sum_{1}^{n}{}_i \sum_{\tilde{i}}{}_{j,k} K_d (\alpha_{ijk} - \alpha^0_{ijk})^2 d^2$$

where the symbol $\tilde{i}$ has been used to mean a summation over the nearest neighbors of the i-th molecule, and d has been introduced to give K_d the same dimensions as K_c.

This potential has been used to compute numerically the vibrational component of the free energy of cubic crystallites with a simple cubic lattice. Crystallites of 8, 27, 64 and 125 molecules have been considered. The 27 molecules cube is shown in fig. 1. The force-constant matrix F is found from the potential Φ:

$$F_{ik} = 1/m \, \partial^2 \Phi / \partial x_i \partial x_k$$

m being the mass of each molecule and x_i, x_k two of the 3n coordinates. The eigenvalues of F are the squares of the ω_i's (see, e.g., ref.[1], p.110). The product of the ω_i^2's (including the six zero values competing to rigid translations and rotations of the whole crystallite) is det F. Obviously, then, detF = 0. With a simple mathematical transformation a matrix F' can be found, which has all the eigenvalues of F except the zeroes. The determinant of F', equal to

$$\prod_{i=1}^{3n-6} \omega_i^2$$

has been computed numerically for several values of the ratio $q = \sqrt{K_d/K_c}$. In order to express the results in a convenient way, let us rewrite eq. (1) as follows:

$$(2) \qquad f_{n,vib} = [-(3n-6) \ln \frac{T}{\Theta} + K] \, kT$$

with: $\Theta = \Omega_c \, h/k$ as a characteristic temperature and:

$K = \ln \prod_{i=1}^{3n-6} [\omega_{ni}/\Omega_c]$. The computed values of K are shown in table 1.

K

q	n = 8	n = 27	n = 64	n = 125
.05	-7.8944	-25.752	-45.658	-66.166
.10	-3.6467	-10.463	-13.500	- 9.784
.15	-1.0708	- 0.803	8.094	30.439
.20	0.8475	6.716	25.784	64.706
.25	2.4209	13.127	41.420	95.667
.30	3.7845	18.858	55.718	124.325
.35	5.0073	24.008	69.019	151.159
.40	6.1278	29.009	81.508	176.448
.45	7.7697	33.610	93.304	200.378
.50	8.1479	37.962	104.489	223.089

TABLE 1

Computed values of factor K of eq. (2) for four cubic crystallites (8 to 125 molecules) and several values of $q = \sqrt{K_d/K_c}$

It is customary (as in ref.[3]) to interpret these results in terms of excess entropy. An Einstein frequency ω_e is defined as the frequency with which an internal molecule would oscillate if the other molecules were fixed. In our case $\omega_e = \sqrt{2\Omega_c^2 + 16\,\Omega_d^2}$, where $\Omega_c = \sqrt{K_c/m}$, $\Omega_d = \sqrt{K_d/m}$. The excess entropy per molecule is then defined as:

$$(3) \qquad S_e = \frac{1}{n} \ln \prod_{i=1}^{3n-6} \frac{\omega_e}{\omega_i}$$

Notice that, if $T_e = h\omega_e/k$ is defined as the Einstein temperature, the vibrational contribution to free energy is:

$$f_{n,vib} = -kT\,[(3n-6)\,\ln T/T_e + nS_e].$$

Figure 3 shows the computed values of S_e versus n. For each given value of q, S_e behaves as expected; it decreases with n, as surface molecules become less and less important than bulk molecules; the downturn for small values of n is due to the "replacement" entropy - that is, substantially, to the fact that six frequencies are missing. What is remarkable is the strong dependence on the ratio q. For q = 0, S_e goes to

infinity. Geometrical considerations show that, in the n-molecules cube, there are $3(n^{2/3} - 2)$ independent non-rigid deformations that involve only distortion of angles, without compression of distances between nearest neighbors. Consequently, $3(n^{2/3} - 2)$ natural frequencies are a function of K_d alone and go to zero when q does, whereas ω_e does not. To avoid this inconvenience, we can introduce another Einstein frequency, depending on K_d alone: $\omega_e' = 4\Omega_d$ and then define a modified excess entropy:

$$(4) \qquad S_e' = \frac{1}{n} \frac{\ln \left[\omega_e^{3(n-n^{2/3})} \; \omega_e'^{3(n^{2/3}-2)}\right]}{\ln \prod_{i=1}^{3n-6} \omega_i}$$

which takes into account the existence of purely distortional and mixed (compressional-distortional) natural modes.

Figure 2 shows S_e' versus n. The dependence on q remains, but, at least, the singularity is avoided. The results are regrettably too few to show a clear law in the dependence of S_e' on q and n, but the general behavior is correct.

It is apparent that the results of a model involving two elastic constants are more difficult to interpret than those of the model of ref.[3] (see their interpretation in ref.[1], p.130 ff.). Yet, a two-constant model is necessary unless we restrict our investigations to the narrow case of f.c.c. lattice. Hopefully, the model proposed here will prove instrumental in broadening the field of data on the free energy of crystallites.

REFERENCES

1. F.F. Abraham, Homogeneous Nucleation Theory, Academic Press, New York, 1974.
2. F.F. Abraham and J. Canosa, J. Chem. Phys., 50, 1303 (1969).
3. W.G. Hoover, A.C. Hindmarsh and B.L. Holian, J. Chem. Phys., 57, 1980 (1972).
4. F.H. Stillinger and A. Rahman, J. Chem. Phys., 55, 1336 (1971).
5. F.H. Stillinger and A. Rahman, J. Chem. Phys., 60, 1545 (1974).

This research was supported by the U.S. Air Force Office of Scientific Research under contract # F44620-76-C-0036.

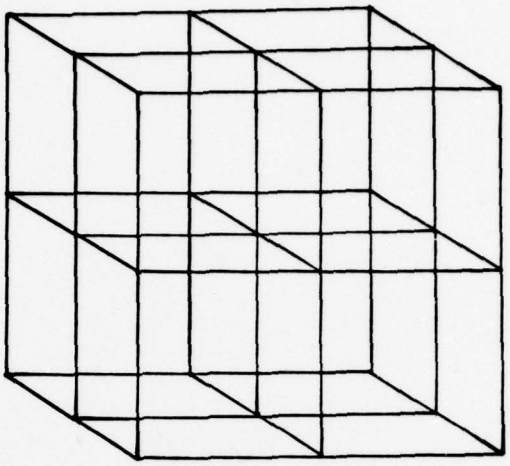

FIGURE 1
Lattice of a simple cubic crystallite of 27 molecules.

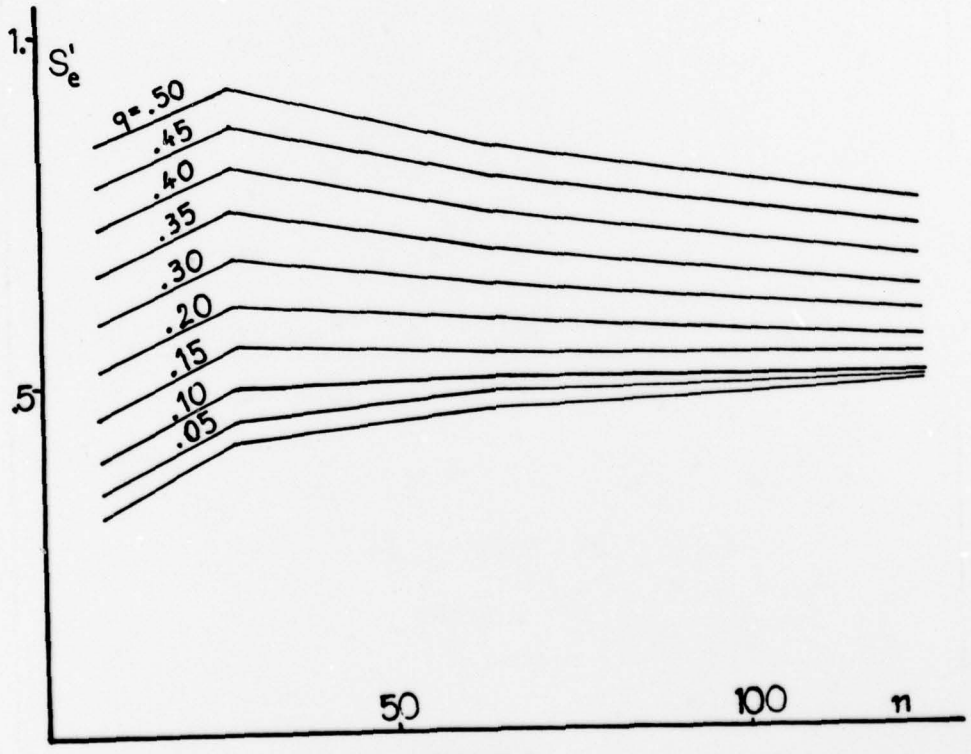

FIGURE 2
Modified excess entropy S'_e vs. crystallite size
for several values of q (eq. 4).

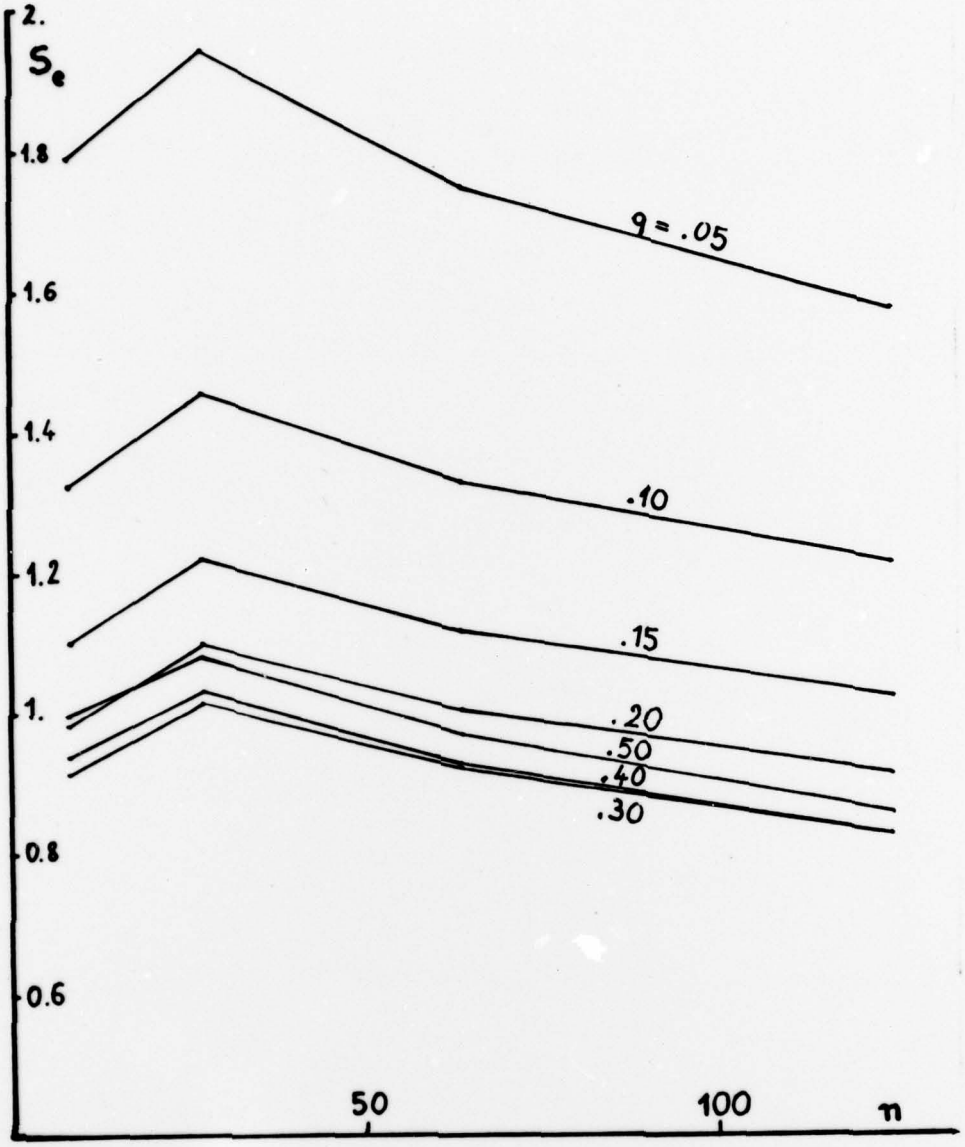

FIGURE 3

Excess entropy S_e vs. crystallite size (eq. 3).

Time-of-Flight Analysis by the Pseudorandom Chopping Technique: Calibration and Application to Mass Spectrometry

David D. Dreyfuss*, Robert B. Doak,[+] Harold Y. Wachman[++]

A time-of-flight apparatus utilizing a cross correlation chopper for beam modulation has been calibrated against a Maxwellian stream. A consistent and reliable scheme for determining the time origin, to ±5 μ sec for any arbitrary time-of-flight wave-form has been devised. It is also shown that the need for deconvolution over shutter function is virtually eliminated, since with this scheme it is possible to work in principle with an arbitrarily narrow width of unit slot. A relatively simple and straightforward analytical procedure for deconvoluting the modulated signal is described.

---

* Present Address: Dept. of Aeronautics & Astronautics, M.I.T., Cambridge, MA

[+]Present Address: Aerodyne Research, Burlington, MA, USA

[++] Professor, Dept. of Aeronautics & Astronautics, M.I.T., Cambridge, MA, USA

1. Introduction

In 1966 we reported [1, 2] from this laboratory, on the calibration and performance of a time-of-flight (TOF) apparatus (fig. 1) in which the shutter consisted of a single rotating disk having four narrow slots of equal widths located at 90° intervals around the rim. The detector consisted of an electron beam ionizer which (ideally) produced a sheet of electrons, which ionized the molecular stream at a plane. The ions were drawn out of the stream and collected on an electron multiplier.

There are several limitations to this scheme. The time resolution of the apparatus is determined by the ratio of the open to closed arc segments around the disk (the chopping period, which is the sum of these two lengths, is fixed by the need to prevent overlap of fast molecules from one pulse and slow molecules of the previous pulse). To obtain good time resolution, one uses a narrow slot. It is, in principle, possible to deconvolute from the effects of a wide slot (shutter function), but the mathematical manipulations involved are very sensitive to the magnitude of the noise in the data. In practice, if the shutter function is broad enough to distort the TOF waveform, then the best that deconvolution provides are the lowest order moments of the velocity distribution represented. Usually, in the past, it was found necessary to sacrifice information on velocity, and use a wide enough slit to transmit a sensible signal in each pulse.

The ionization detector has its own limitations. An electron beam ionizer is a universal detector, hence is usable for all molecular species in the test stream. As a consequence, however, background molecules are detected as well (in particular, with permanent gases, all those stream

molecules which strike closed portions of the disk are detected as background). Statistical fluctuations in this background are usually the major source of noise in the TOF data. Other detector problems include the finite extent of the ionization region along the beam direction and non-zero ion travel time between the instant of ionization and detection. The extent of the ionization region does not present a serious problem because it has only a second order effect on the TOF distribution (the finite shutter function is a first order effect). We have shown [3] that a considerable flight path through the ionization region (up to about 25% of the total flight path) can be used before appreciable distortion in waveform occurs, and we have taken advantage of this to improve the efficiency of ionization. As to the effects of the ion travel time, it can be made insignificant with sufficient draw-out potentials or alternatively it can be accounted for in interpreting the data.

2. Pseudorandom Chopping

An alternative approach to molecular beam chopping, which avoids many of the problems cited above is to use a pseudorandom chopping scheme (fig. 2). This technique was originally developed in connection with thermal neutron studies [4-7], and has only recently been used with neutral molecular beams [8, 9]. In comparison to the scheme described above a larger number of pulses of molecules are produced over each revolution of the disk. As a consequence several pulses are produced

within each chopping period, which overlap at the detector. By spacing the pulses "randomly" within the period, it is possible by a simple arithmetic procedure to undo the overlap produced [3, 9]. It is possible, in fact, to attain a duty cycle of 50% for such a chopper independent of individual slot width. With this chopper, the time resolution is determined by the length of the pseudorandom chopping sequence, where "length" counts the total number of unit slot widths (note that several adjacent locations may be open, thus forming a single larger slot which is treated as a set of unit slots). The deconvolution procedure recovers the waveform which would be obtained from a chopper with a single unit slot per period. While it is conceivable, in principle, to improve time resolution arbitrarily by taking longer and longer sequences, in practice, limitations in electronic response time and the need to have unit slot width compatible with molecular beam width precludes this extension. Avoiding these problems by using larger diameter disks will cause other experimental difficulties. (Given an electronic chopping scheme of some sort (e.g. chopping laser excitation of a beam), this last limitation may not apply, since chopping could be entirely independent of collimation, and even better time resolution might be obtainable.)

3. Calibration

Although the pseudorandom chopping technique has been demonstrated for molecular beams, to our knowledge, no calibration of a system using the technique has been reported. We have performed such a calibration against inert gas Maxwellian beams. A schematic diagram of the apparatus is shown in figure 3. A room temperature gas reservoir at a pressure on

the order of 10 Pa supplies a beam through a small hole in a thin stainless steel wall. In operation, conditions were such that adequate signals were achieved for a source Knudsen number, Kn $\sim$ 1. Flow at this value of Kn is perhaps not fully molecular (one would like to use Kn $\simeq$ 100), but it appears adequate for velocity distribution measurements from comparison of velocity distributions for a series of decreasing source pressures which indicates no measurable change in distribution when values of Kn $\gtrsim$ .1 are used.

Some examples of calibration runs are shown in figure 4. To compare the data with the known velocity distribution of the gas in the source, a least square fit of a Maxwellian velocity distribution to the data was made. Source parameters such as molecular weight and temperature which are known or independently measurable were held fixed. Fitting parameters were a baseline position (baseline information is lost experimentally because the signal is superposed on a large DC background), and an overall amplitude factor. The distribution is linear in these quantities, so the fitting is straight-forward and well-defined. It avoids the hazards of peak height matching in that it weights all data points equally, and can be used for comparison with moderately noisy data. Also it is readily extended to gas mixtures, which should have a velocity distribution consisting of a weighted sum of two different Maxwellians.

4. Time Origin Considerations

One parameter important to comparison of the data with Maxwellian theory, which has not so far been mentioned, is the location of the time origin in the TOF waveform. Physically, this is the time at which all

molecules represented by the TOF waveform passed the chopper. Because of the sharp leading edge of the Maxwellian TOF waveform, small differences in time origin (less than one channel (slot) width or 15 μsec) are readily detected. In making a calibration it is especially important that the time origin be fixed independently, and not determined by matching peak locations or the leading edge or by some similar scheme.

In principle, the time origin is easy to determine. Using a photo-trigger reference, whose position relative to the beam position is measured, time origin can be determined in terms of some constant number of channels. Time delays associated with either ion drawout time or electron signal processing, are essentially constant, and may also be assessed. It is difficult, however, to measure these delays independently with sufficient precision. It seems best to measure them for the composite apparatus. Of the several schemes attempted, the following appeared the most satisfactory.

Using the complete system with molecular beam and all processing electronics in place, electronic delays were determined from background gas detection without the chopper. For this process the electron accelerating grid in the ionizer was pulsed electronically, and the time delay from the electronic pulse to signal rise was measured. To determine geometric timing relationships, a series of TOF spectra were measured for a constant intense signal. (The stream was not necessarily Maxwellian: we used a fairly high pressure H_2O beam for which we could obtain an excellent signal-to-noise ratio.) These TOF waveforms were produced by rotating the chopper both "forward" and "backwards" (the relative location of the photo-trigger and molecular beam define directions). Then the relative location of some

known feature (e.g. peak position) for the two resulting waveforms were compared to give a measure of the geometric timing relationship which is independent of electronic delays. Improved precision in the measurement can be obtained by making the measurement at several chopping frequencies. We have been able to locate the time origin to within about ±1/3 channel (typically ± a few microseconds for our operating chopping period of 1-2 msec and pseudorandom sequence of length 103) using these techniques.

5. Applications to Mass Spectrometry

One possible application of the improved resolution TOF system we have developed is to mass spectrometry (see fig. 5). As mentioned above in connection with the fitting of theoretical curves to the data, it is possible to obtain a measure of the relative amounts of gases in a gas mixture by comparing amplitude of the fitting Maxwellians. The advantage of the technique is that it is non-destructive, in the sense that ionization takes place only after the necessary information (time of flight between two fixed points) has been obtained. There are difficulties, however, because the velocity distributions for the species to be separated must be known independently. This information is available, *a priori* only for free molecular flows. If Maxwellian velocity distributions must be used, only a few fairly widely spaced molecular weights can reasonably be separated since the separate TOF peaks are broad and overlapping. In some experimental situations, for example, detection of dimers and higher order clusters in near condensing systems, the advantage of non-destructive sensing may outweigh the disadvantages cited.

REFERENCES

1. P. B. Scott, "Molecular Beam Velocity Distribution Measurements" M.I.T. Fluid Dynamics Research Lab. Report 65-1, Cambridge, MA, (1965).

2. P. B. Scott et al., in RGD (C.L. Brundin ed.) p. 1353, Academic Press New York, (1967).

3. David D. Dreyfuss, "Neutral Time of Flight Mass Spectrometry," SM Thesis, M.I.T., Cambridge, MA (1977).

4. T.E. Stein, et al., J. Nuc. Energy A/B 16, 499 (1962).

5. K. Sköld, Nucl. Instr. and Meth. 63, 114 (1968).

6. A. Virjo, Nucl. Instr. and Meth. 73, 189 (1969).

7. W. Gläser and F. Gompf, Nukleonik 12, 153 (1969).

8. V. L. Hirschy and J. P. Aldridge, RSI 42, 381 (1971).

9. H. D. Meyer, Max Planck Inst., Göttingen Bericht 113 (1974).

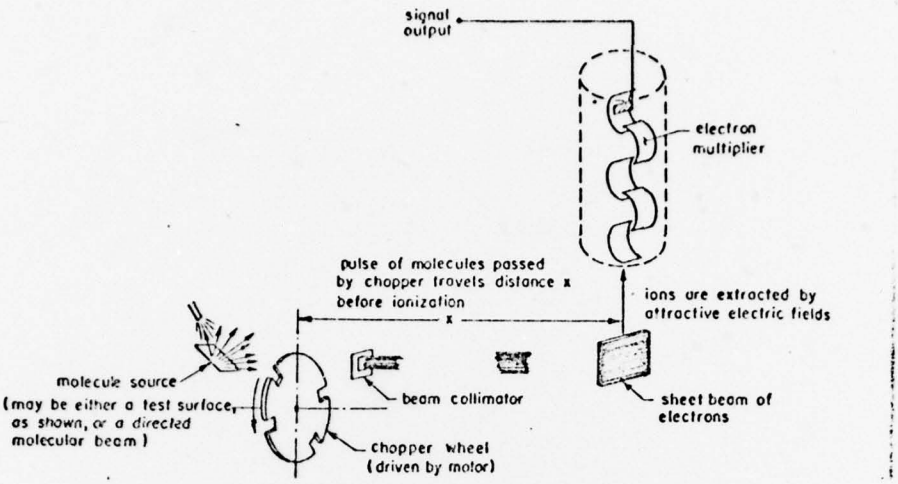

FIGURE 1

Typical TOF Apparatus

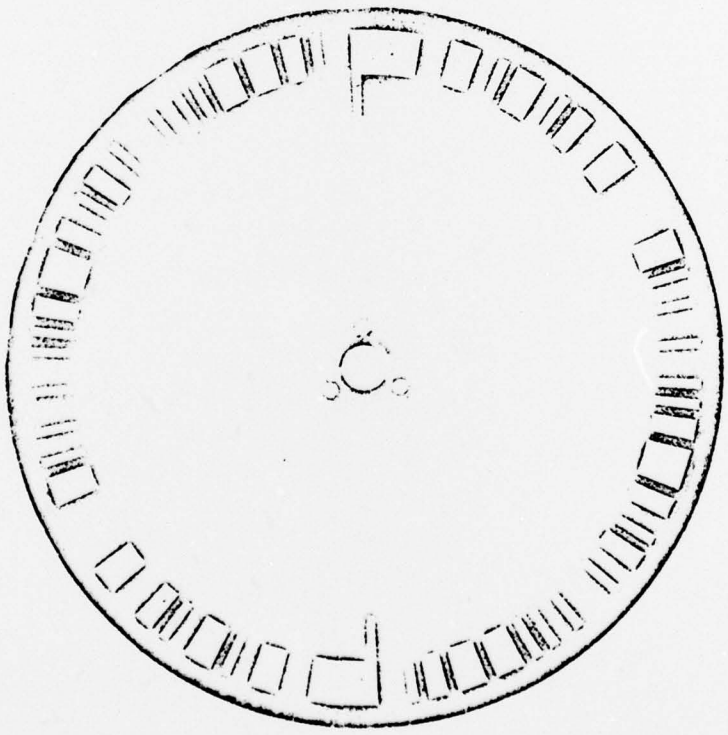

FIGURE 2

Pseudorandom Chopper

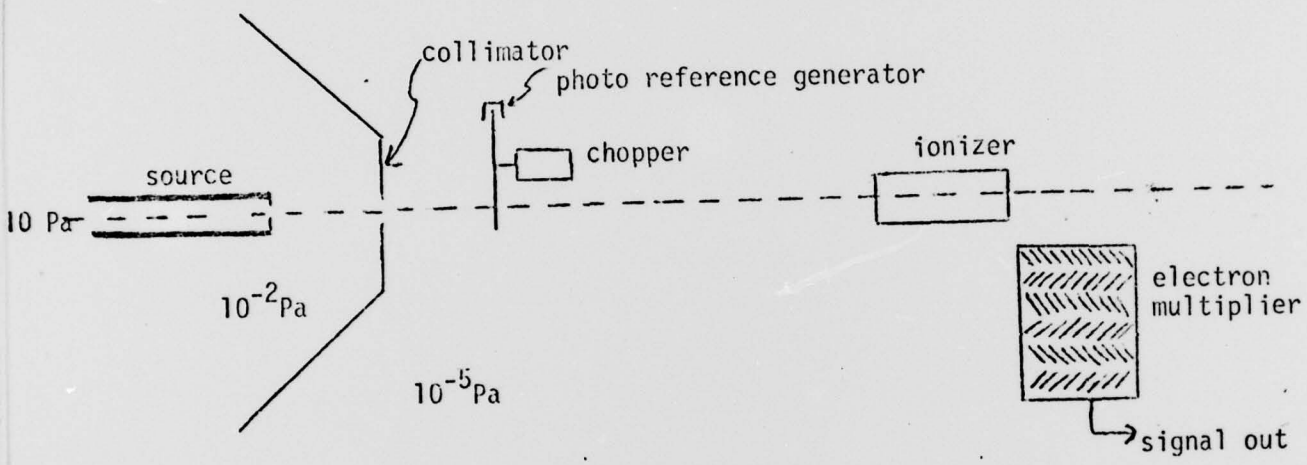

FIGURE 3
The Apparatus

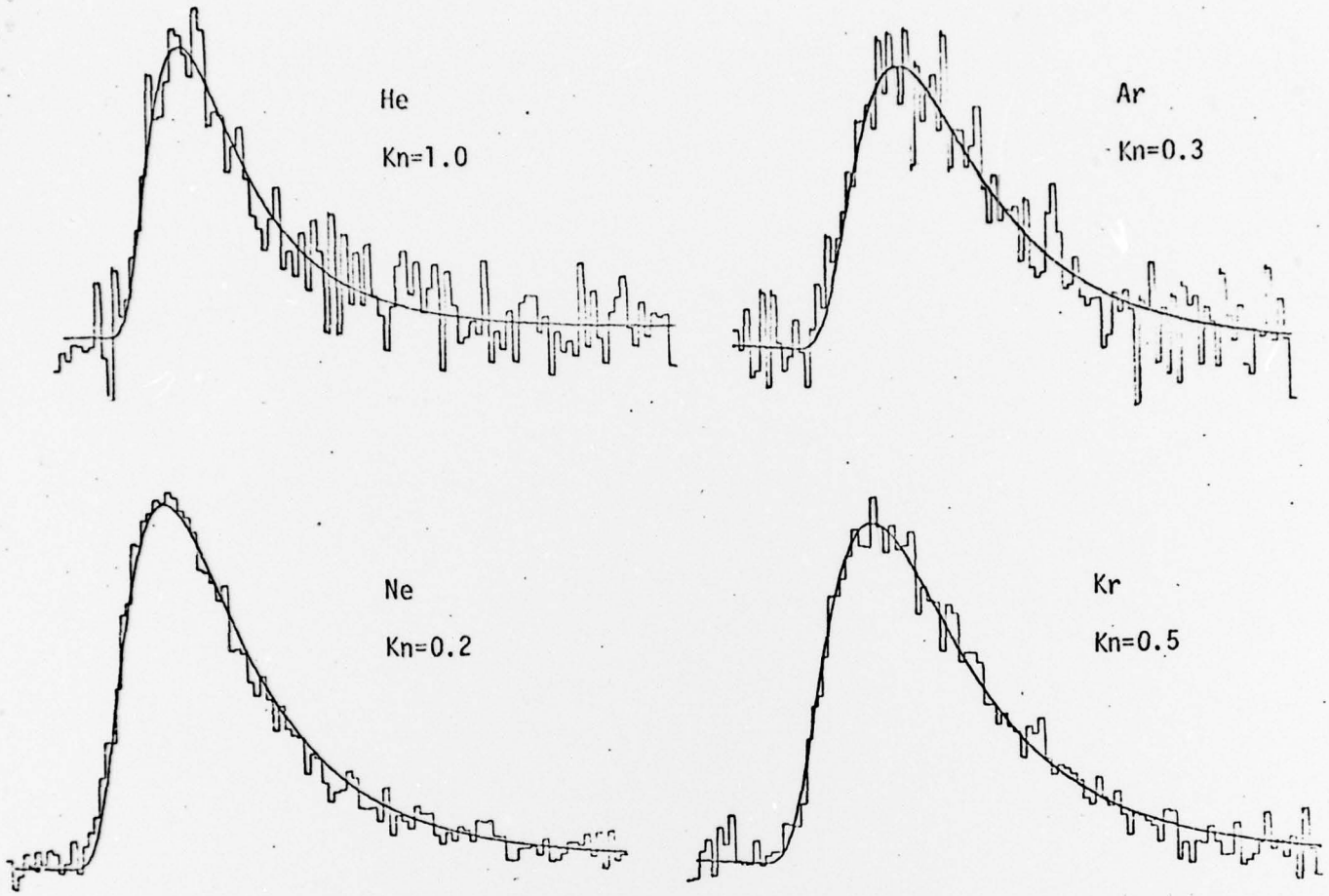

FIGURE 4

Calibration Examples

Solid Curves are theoretical Maxwellian TOF curves at source temperature (fitting parameters: baseline, amplitude). Periods (abscissas) are not equal.

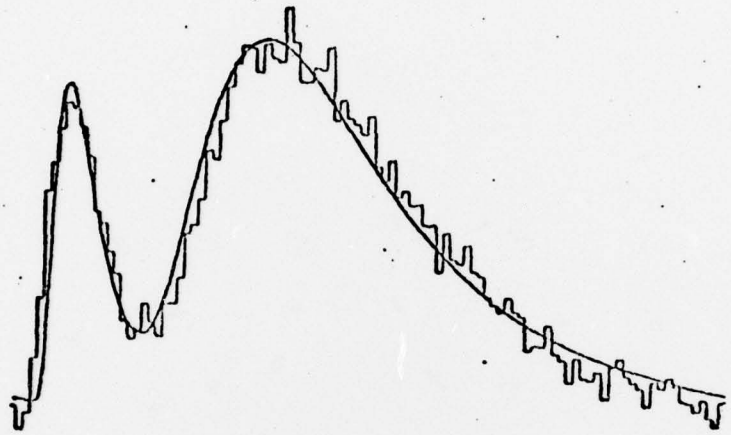

FIGURE 5

Sample TOF Waveform for a H_2/Ar Gas Mixture. Solid Curve is a least-squares fit of a sum of two Maxwellians to the data (fitting parameters: baseline, amplitudes).